ACS NANO

www.acsnano.org

PERSPECTIVE

Mass Transfer Analysis for Achieving High-Rate Lithium–Air Batteries

Yu-Long Liang, Yue Yu, Zi-Wei Li, Jun-Min Yan, Gang Huang,* and Xin-Bo Zhang*

Cite This: *ACS Nano* 2024, 18, 17361–17368

Read Online

ACCESS | Metrics & More | Article Recommendations

ABSTRACT: **Lithium–air batteries (LABs) have aroused worldwide interest due to their high energy density as a promising next-generation battery technology. From a practical standpoint, one of the most pressing issues currently in LABs is their poor rate performance. Accelerating the mass transfer rate within LABs is a crucial aspect for enhancing their rate capability. In this Perspective, we have meticulously analyzed the ion and oxygen transport processes to provide readers with a comprehensive understanding of the mass transfer within LABs. Following this, we have discussed potential misconceptions in the existing literature and propose our recommendations for improving the rate performance of LABs. This Perspective provides a deep insight into the mass transfer process in LABs and offers promising strategies for developing other high-rate metal–O_2 batteries.**

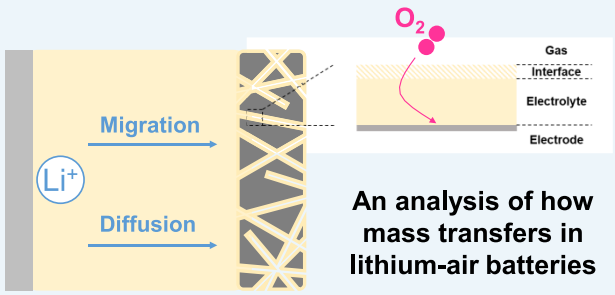

KEYWORDS: *lithium–air batteries, rate performance, mass transfer, tip effect, potential distribution*

INTRODUCTION

Lithium–air batteries (LABs) have the highest theoretical energy density among existing rechargeable battery systems. They have been heralded as a promising next-generation energy storage system for applications such as electric vehicles (EVs). However, due to their poor rate performance, it is difficult for them to meet the increasing power demands of EVs. Currently, the most widely used batteries on EVs are lithium-ion batteries (LIBs), which exhibit minimal overpotential and acceptable capacity decay during discharge even at a C-rate higher than 10 C,[1−8] corresponding to the area current density from several to tens of mA cm^{-2}. In comparison, the typical current density for testing LABs is only ∼0.1 mA cm^{-2}, and the overpotential tends to increase rapidly as the current increases to several mA cm^{-2} (batteries would even fail within seconds). This means to achieve the same output power, the volume of LABs packs is at least an order of magnitude larger than that of LIBs. Therefore, if LABs target applications with broad markets such as EVs, the rate performance of these batteries must be significantly improved.

It is widely accepted that the poor rate performance of LABs is primarily attributed to the sluggish mass transfer process, rather than the kinetics of electrode reactions.[9−12] To this end, researchers can propose effective solutions to enhance the rate performance of LABs only after acquiring a comprehensive understanding of the mass transfer process. However, there is limited literature in the field of LABs focusing on mass transfer. The discussion of mass transfer in existing articles tends to individually emphasize the impact of various battery parameters on mass transfer.[13] These discussions focus too much on the details and lack a description of the entire mass transfer process.

In this Perspective, we aim to provide a comprehensive understanding and promote the commercialization of LABs by discussing the intricacies of mass transfer during different processes. Mass transfer in LABs involves the transfer of oxygen and ions. Starting from discussing the electric field distribution within the battery, we carefully analyzed the ion transfer in different battery regions. Inside the cathode, the process of oxygen transfer is divided into three distinct stages, and each stage is briefly analyzed. In the discussion of mass transfer when discharge products exist, we found that it is closely related to the interface where the electrode reactions occur. Finally, some promising suggestions for enhancing the rate performance of LABs are provided.

Received: April 5, 2024
Revised: May 26, 2024
Accepted: June 5, 2024
Published: June 24, 2024

https://doi.org/10.1021/acsnano.4c04529
ACS Nano 2024, 18, 17361–17368

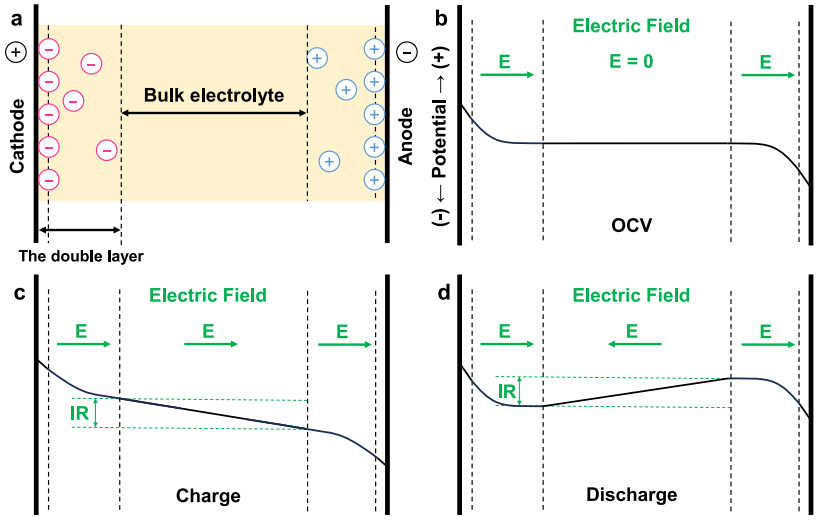

Figure 1. (a) Illustration of the regions within a LAB. Potential distribution of a LAB at the (b) open circuit voltage (OCV) state, (c) charge state, and (d) discharge state.

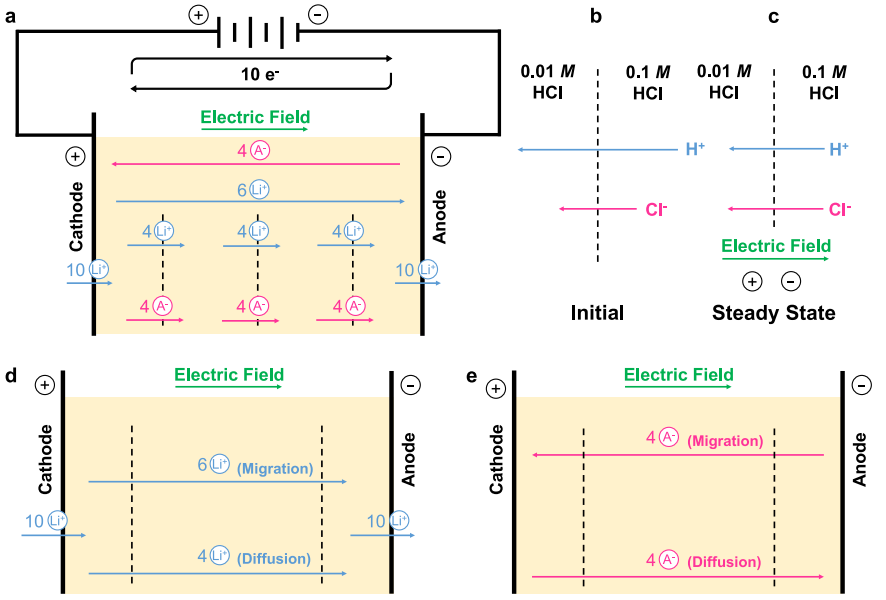

Figure 2. (a) Schematic diagram of the circuit structure and ion transfer during the charge process. The dashed lines represent the hypothetical interfaces used to illustrate the movement of ions between different regions. (b, c) Illustrations of the formation process of the liquid junction potential. The transfer of (d) cations and (e) anions.

ION TRANSFER IN THE BULK ELECTROLYTE

The transfer of ions in batteries typically comprises three components: diffusion, electromigration, and convection. For most LABs, convection is negligible. Therefore, we only have to deal with migration and diffusion. The driving force for electromigration is the electric field, and for diffusion, it is the concentration gradient. Before a discussion of electromigration, the electric field distribution within the LABs should be clarified first. The electric field E between two parallel electrodes carrying opposite charges can typically be calculated by $E = U/d$, where U is the potential difference between the two electrodes and d is the distance between them. When there is an electrolyte between the two electrodes, the influence of electrolyte as a dielectric on the potential distribution must be taken into consideration (Figure 1a). The macroscopic dielectric constant of the electrolyte is not equal to that of the solvent, as the addition of solutes could significantly increase the dielectric constant of electrolytes.[14,15] At the OCV state, the potential drop occurs entirely at the interfaces between the electrodes and the electrolyte, namely, the double layer (Figure 1b). Meanwhile, the potential in the bulk electrolyte remains constant. As depicted in Figure 1c, during the charge process, the concentration of Li^+ near the cathode increases as a result of the decomposition of lithium peroxide. And the concentration of Li^+ near the anode decreases due to the reduced potential. Eventually, an electric field is formed in the bulk electrolyte, directed from the cathode to the anode. During the discharge process, an electric field in the opposite direction is formed due to the opposite causes (Figure 1d). The potential drop across the bulk electrolyte, labeled as "IR", increases with the current. The direction of the electric field in the bulk electrolyte changes with the battery's state. However,

https://doi.org/10.1021/acsnano.4c04529
ACS Nano 2024, 18, 17361−17368

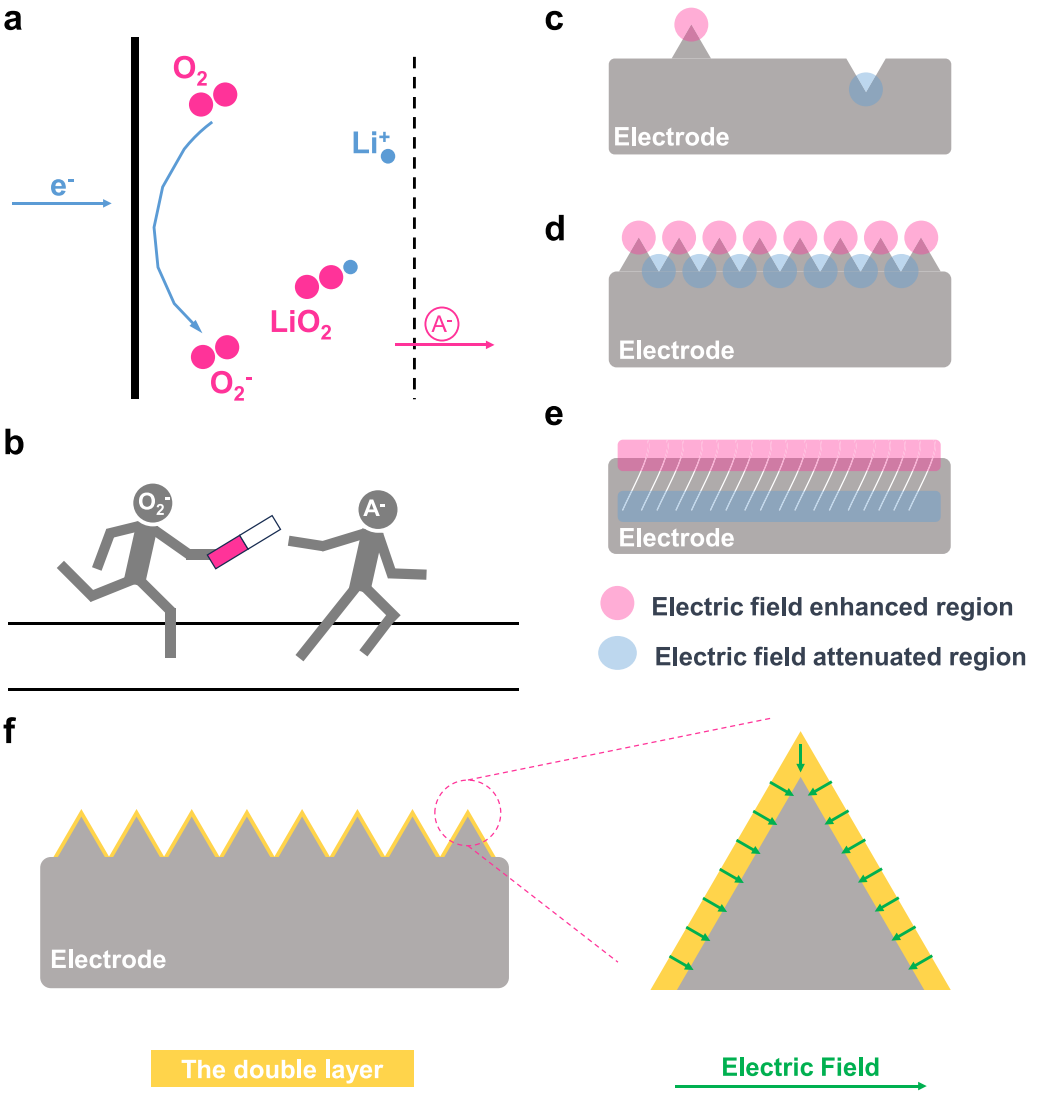

Figure 3. (a) Schematic diagram of the current carried by superoxide ions. (b) Illustration of the transformation of carriers. (c–e) Reasoning about the electric field inside the electrode if the tip effect is significant. (f) Possible electric field distribution at electrode surface protrusions in high-concentration electrolyte.

in the double-layer region, the direction of the electric field always goes from the cathode to the anode.

To discuss the ion migration process in LABs that have reached the steady state (the potential distribution does not change with time), the concept of migration number (t) must be introduced. This concept helps distinguish the contribution of each kind of ion to the total current. For simplicity, we have just considered a situation in which there is only one kind of cation and one kind of anion in the electrolyte, with each ion carrying only one unit of charge. t_+ and t_- are used to represent the migration numbers of the cation and anion, respectively. Figure 2 depicts the ion transfer within the bulk electrolyte. As shown in Figure 2a, during the charge process, the direction of the electric field is from the cathode to the anode. Assume that t_+= 0.6, and a total current equivalent to 10 e^- per unit time passes through the cell. The total current is carried in the bulk electrolyte by the movement of 6 Li^+ and 4 anions. Ideally, anions are inert, and 10 Li^+ ions are reduced at the interface between the anode and electrolyte. However, through migration, only 6 Li^+ ions reach the interface, and the remaining 4 Li^+ ions required are supplemented by the diffusion. For diffusion, four anions must move along with cations; otherwise, the potential distribution of the electrolyte will be changed, which contradicts our steady state assumption. To illustrate this, we give the following example: the potential drop caused by the different diffusion rate of ions is defined as the liquid junction potential. The formation process of the liquid junction is shown in Figure 2b,c. Due to the concentration gradient, H^+ and Cl^- will move from the right to the left. However, the diffusion rate of H^+ is higher than that of Cl^-, resulting in the accumulation of positive charges on the left side. These charges would form an electric field from left to right, which inhibits the movement of cations and promotes the movement of anions until them cross the boundary at equal rates.

In the area close to the cathode, oxidation reactions occur. Ten Li^+ ions enter the electrolyte from the solid phase: six of them move toward the anode driven by the electric field, while the other four cations are driven by the concentration gradient. Figure 2d,e illustrates the motion of cations and anions, respectively. For Li^+, there is a balance between the reaction rate at the interfaces and the mass transfer rate in the

https://doi.org/10.1021/acsnano.4c04529
ACS Nano 2024, 18, 17361−17368

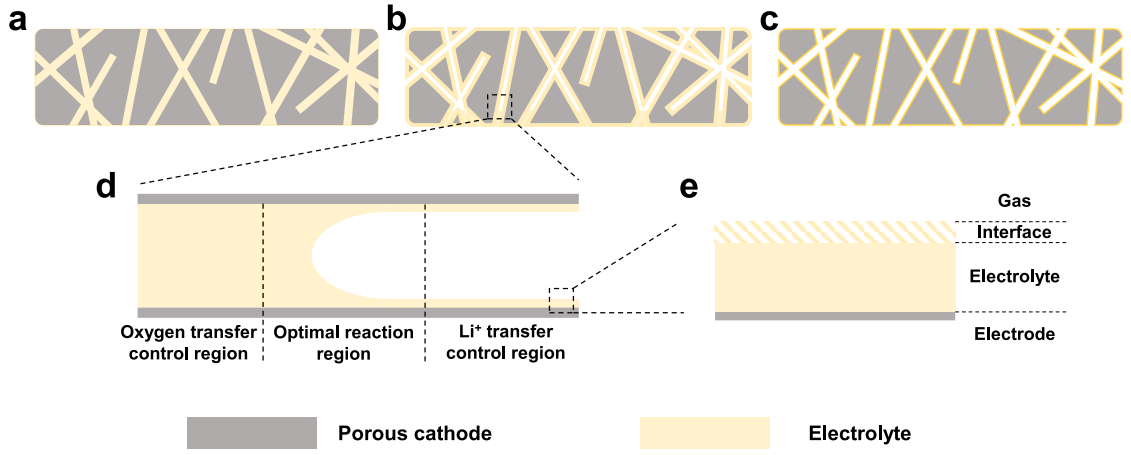

Figure 4. Schematic diagram of the infiltration state of cathode: (a) flooded; (b) wetted; (c) dry. (d) Illustration of the triple-phase interface. (e) The three stages of oxygen transfer.

electrolyte. For anions, this means that the electromigration rate equals the diffusion rate but in opposite directions. The anions appear to circulate between the anode and the cathode. During the discharge process, due to the reversal of the electric field direction in the bulk electrolyte and the occurrence of reverse reactions on the electrodes, the movement of all of the ions mentioned above will be reversed. It should also be noted that the solution environment may affect the above conclusions. An extreme example is that the zinc ions exist in the form of Zn^{2+} when pH $\leq$ 8 and in the form of $Zn(OH)_4^{2-}$ when pH $\geq$ 12. The different charges of zinc ions, positive or negative, may change the direction of ion migration.

Next, the situation when the battery is charged at a higher rate has been discussed. Assuming that 100 electrons pass through the circuit in a unit of time, each number in Figure 2a increases 10-fold, but the proportion between these numbers remains the same (assuming the migration number remains unchanged). A higher current requires a higher overpotential, and the increased overpotential would not only accelerate the reaction rate on the electrodes but also expand the potential difference across the bulk electrolyte. The transfer rate of Li^+ moving through the electromigration will continuously increase with the increase of overpotential. While the mass transfer rate cannot infinitely increase by augmenting the overpotential, this is because there will always be a significant proportion of ions that must be transferred through the diffusion. Once the maximum diffusion rate cannot meet the requirements, the battery will fail. Therefore, when selecting an electrolyte for better ion transfer efficiency, one should at least consider the following aspects: ion conductivity (determining the ease of Li^+ migration), migration number (determining the proportion of Li^+ migration and diffusion), ion diffusion coefficient, and solubility of lithium salts (determining the ease of Li^+ diffusion). For solid electrolytes, the transfer of Li^+ occurs only through the migration, but their ionic conductivity is usually much smaller than that of liquid electrolytes.

It is worth noting that, particularly for the solution-mediated mechanism, the superoxide ions generated during the oxygen reduction in LABs could also function as current carriers (Figure 3a). The distance that superoxide ions can move away from the cathode surface depends on the characteristics of the electrolyte. As superoxide ions react with Li^+ to form electrically neutral lithium superoxide, their role in carrying current is gradually replaced by the anions of the lithium salt. The chemical reaction in this process operates similarly to the passing of a relay baton among athletes in a relay race (Figure 3b).

MASS TRANSFER INSIDE ELECTRODES

After discussing the transfer of ions in the bulk electrolyte, the ion transfer inside the electrodes has been taken into consideration, which has been analyzed starting with the discussion of "tip effect" and then the electric field distribution inside the electrodes. Some researchers posit that the presence of sharp tips on the electrode surface enhances the local electric field and promotes mass transfer. However, this viewpoint is not comprehensive, since the tip effect is a function of curvature. As shown in Figure 3c, regions with positive curvature experience enhanced electric field intensity, while the electric field is weakened in regions with negative curvature. Further ratiocinating from Figure 3c, the following conclusion can be drawn. If there is a significant tip effect in the battery, then the electric field inside the porous electrode will be greatly weakened (Figure 3d,e). Consequently, the transfer of ions within the electrode will be almost unaffected by the electric field and will rely primarily on the diffusion. This conclusion seems to align with the Gauss law, which states that the excess charges in a conductor will be entirely concentrated on its surface. However, it does not account for the situation where electrolyte exists. Typically, the influence of ions in the electrolyte on the electric field distribution needs to be considered using Boltzmann distribution and the Poisson equation, as is done in electrochemistry when dealing with the double layer. The characteristic thickness of the double layer is related to the concentration of the electrolyte. For 1 M electrolyte, it is around 3.0 Å (approximately equal to the diameter of 2 to 3 Li^+).[16] As we discussed above, when the battery is at the OCV, the potential drop is entirely concentrated in the double layer. This means that in high-concentration electrolytes, the electric field will be distributed almost uniformly on the electrode surface, as shown in Figure 3f. This inference is consistent with the calculation results reported by Andrews et al.[17] The thickness of the double layer will gradually increase to approximately 9.6 Å as the electrolyte concentration decreases to 0.1 M. From this point of view, we believe that the tip effect on the surface of electrodes is significant only when the overpotential is quite large and the surface concentration of ions is extremely low. In summary, the

https://doi.org/10.1021/acsnano.4c04529
ACS Nano 2024, 18, 17361−17368

potential distribution inside the electrode is closely related to the construction of the double layer. It should be noted that the steric effect of anions may also influence the double layer on the cathode side. The anions of commonly used lithium salts in LABs are usually large in size, and it is difficult for them to enter the tiny pores or thin electrolyte layers. This could be supported by the Randles−Sevcik equation usually used in LIBs. The Randles−Sevcik equation, derived from electrode dynamics and diffusion processes, shows that the transfer of Li^+ inside the layered materials is not driven by the electric field.

The mass transfer inside the cathodes of LABs is also significantly influenced by the amount of electrolyte added. It is generally believed that an excess of electrolyte could inundate the cathode, impeding oxygen transfer and weakening the rate performance of LABs (Figure 4a). Nevertheless, insufficient electrolyte could lead to difficulties in Li^+ transfer, reduced electrode reactive areas, and other issues (Figure 4c). The ideal electrolyte quantity can be depicted in Figure 4b: there is an abundance of triple-phase interfaces within the cathode, which is considered beneficial for the full liberation of the discharge capacity of LABs. Figure 4d illustrates one of the triple-phase interfaces in the cathode side, which can be divided into three regions: the oxygen transfer control region, the optimal reaction region, and the Li^+ transfer control region.[18] It is worth emphasizing that the Li^+ transfer control region may not be described simply by the solution impedance (jR_s). As discussed above, the Li^+ transfer in a thin electrolyte is hardly driven by the electric field. We strongly recommend researchers to emphasize the quantity of electrolyte addition and the infiltration state of the cathode in their papers. Otherwise, comparisons between conclusions from different articles may be challenging.

MASS TRANSFER OF OXYGEN

In LABs, there are primarily two differences between the transfer of oxygen and Li^+. One is that Li^+ carries positive charge, while oxygen is electrically neutral. This means that the transfer of oxygen in the liquid phase is not influenced by the electric field and is solely driven by the concentration gradient. The other difference is that the oxygen transfer involves crossing from the gas phase to the liquid phase, while the transfer of Li^+ occurs only within the liquid phase. As illustrated in Figure 4e, the process of oxygen transfer can be divided into three distinct stages: the transport from the gas phase to the interface, the passage through the gas−electrolyte interface, and the migration within the liquid phase toward the electrode surface. In the gas phase, the oxygen moves in forms of both diffusion and convection, which are much faster than the transfer rate of oxygen in the liquid phase (in terms of diffusion alone, the diffusion rate of oxygen in the gas phase is 4 orders of magnitude higher than that in the liquid phase).[13] Therefore, the transfer rate of oxygen in the gas phase has little influence on the overall oxygen transfer rate. To distinguish the effects of the latter two stages on the overall oxygen transfer rate, a setup similar to that developed by Zhang et al.[19] is helpful. Continuously adding electrolyte after the electrolyte completely submerged the cathode has no impact on the gas−liquid interface. If the passage of the interface is the rate-determining step of the overall oxygen transfer, additional electrolyte will not significantly affect the current.

The transfer of oxygen within the electrolyte is usually described by Fick's first law, which states that the oxygen transfer rate is related to the diffusion coefficient and oxygen concentration. The two factors, diffusion coefficient and oxygen concentration, are mainly determined by the solvent. In LABs, the most commonly used solvents are dimethyl sulfoxide (DMSO) and tetraethylene glycol dimethyl ether (TEGDME). Gittleson et al.[12] have collected the physical properties of different electrolytes. The oxygen solubilities in DMSO and TEGDME are 0.330 and 0.857 mM, respectively, and the oxygen diffusion coefficient in DMSO is an order of magnitude larger than that in TEGDME. Judging from the rate performance that researchers have achieved, DMSO-based electrolytes are generally more suitable for high-rate LABs.[20] Additionally, Gittleson et al. have also highlighted that the choice of salt species and concentration has a significant influence on oxygen solubility. For example, the oxygen solubility in 1.0 M $LiNO_3$/DMSO is 0.119 mM and in 1.0 M LiTFSI/DMSO is 0.252 mM, which will decrease to 0.209 mM when the concentration of LiTFSI decreases to 0.5 M. For the temperature effect, increasing temperature is believed to reduce the viscosity of the electrolyte and promote the thermal movement of molecules, thereby increasing the diffusion coefficient of oxygen.[10,21,22] However, the solubility of gases in liquids generally decreases as temperature increases, and oxygen is no exception.[23] Besides, increased temperature will also bring about changes in surface tension that will affect the reaction area on the cathode. In short, careful experiments should be designed to avoid the influence of irrelevant factors on oxygen transfer as much as possible.

MASS TRANSFER WHEN DISCHARGE PRODUCTS EXIST

The actual reaction site of the discharge process in LABs, whether it occurs at the interface between the discharge products and electrolyte or at the interface between the electrode and electrolyte, is still a matter of debate. This question also impacts the mass transfer process: If it occurs at the interface between the electrode and electrolyte, both Li^+ and oxygen must pass through the crevices among discharge products. For LABs, the discharge profile typically shows a relatively flat plateau, followed by an abrupt polarization region (known as the "sudden death"). It is generally recognized that the rapid electrochemical polarization stems from the rising impedance at both the anode and cathode.[24] This viewpoint can be traced back to the research conducted by Luntz et al.[25] They have revealed that the charge transport during the discharge process is dominated by tunneling of holes, and this gives a natural explanation for a critical thickness of discharge products to support the electrochemistry. This work suggests that the electrode reaction occurs at the interface between the lithium peroxide and electrolyte rather than at the interface between the electrode and electrolyte, which may not necessarily reflect the actual situation. Furthermore, in practical LABs, the discharge products gradually cover the electrode surface, implying that the impedance of the cathode increases during the discharge process. Therefore, if charge transfer is the rate-determining step in the late stages of LABs' discharge, there should not be a sudden change in potential during constant current discharge.[26] From another point of view, the work of Luntz et al. has demonstrated the challenges of oxygen reduction at the interface between the discharge products and electrolyte, and the real reaction interface is more likely to be close to the electrode. With the help of in situ small- and wide-angle X-ray scattering (SAXS/WAXS) characterization, Freunberger et al.[27] have arrived at the conclusion that the

https://doi.org/10.1021/acsnano.4c04529
ACS Nano 2024, 18, 17361−17368

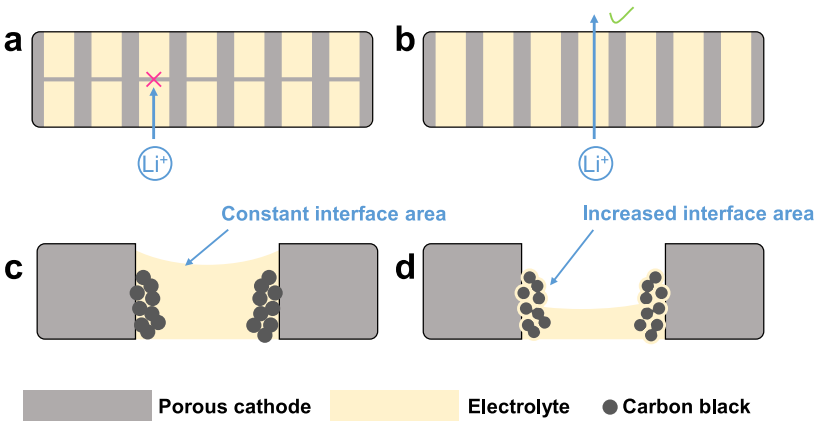

Figure 5. Mass transfer when all of the pores in the cathode are (a) blind holes and (b) through-holes. The cathode materials (c) completely submerged in the electrolyte with constant gas−liquid interface and (d) partially submerged in the electrolyte with increased gas−liquid interface.

mass transport of reactive species through a Li_2O_2 film limits the discharge capacity. This conclusion is also based on the premise that oxygen reduction occurs at the interface between the electrode and electrolyte.

STRATEGIES FOR ENHANCING MASS TRANSFER

To enhance the mass transfer in LABs, strategies, including designing cathode structures and using electrolyte additives, have been adopted. Reasonable pore construction is crucial for cathode materials of LABs. As mentioned previously, the Li^+ transfer in small pores is primarily driven by the concentration gradient. In addition, due to the necessity of accommodating discharge products, the cathode materials must have a sufficiently high porosity. Previous studies have demonstrated that the mesopores (2−50 nm in width) are most conducive to enhancing the discharge capacity of batteries.[28−30] In the work of Gaya et al.,[31] they have investigated the feasibility of using a biporous cathode for improving the electrochemical cell response. To improve the diffusion within the electrode, an extra-macroporosity (width >50 nm) was introduced to serve as the oxygen reservoir and facilitate the oxygen diffusion across the electrode. Besides pore size, the connectivity or permeability of cathode pores should also be considered. As shown in Figure 5a,b, the two cathodes have similar porosity, specific surface area, and pore diameter. The last one can support the oxygen and ion transfer well, while that cannot happen in the first one at all. The connectivity of pores is typically described by the Gurley number, which is currently often used in the research of separators.[32,33] For LABs employing free-standing cathodes, testing the Gurley number is meaningful. Since freestanding cathodes are usually custom-made, twisted or blind-hole pores in these materials may hinder efficient mass transfer. Although significant works have been done on the design of cathode pore structures, the current density that the LABs could endure is still low. Additional cathode architecture design is still highly required for constructing high-rate LABs.

In LABs, it is beneficial to determine which one is the rate-determining step of oxygen transfer: the process through the gas−liquid interface or diffusion in the liquid phase. If the former is identified as the rate-determining step, then the issue can be alleviated by appropriately increasing the specific surface area of the cathode material. A lot of research has already been done to study the impact of cathode specific surface area on the battery performance.[20,34,35] Sun et al.[36] have found that the main factor determining the battery performance is the specific surface area of the mesopores in the carbon-based cathode. As shown in Figure 5c,d, increasing the specific surface area of the cathode material can enlarge the contact area between the gas phase and the electrolyte when the electrode is in an appropriate wetting state. Moreover, the mass transfer across the gas−liquid interface can be increased by adding nanoparticles to the electrolyte. This is due to the nanoparticle induced shuttle effect, mixing of the gas−liquid boundary layer, and inhibition of bubble coalescence.[37] If diffusion in the liquid phase is the rate-determining step, an effective method is introducing electrolyte additives. Perfluorinated chemicals are commonly used as oxygenated additives in LABs. For example, Wu et al. have designed the solution-phase additive 3[2-(perfluorohexyl)ethoxy]-1,2-epoxypropane (FC) to enhance the mass transfer of O_2 in the electrolyte.[38] Yazami et al. have investigated the properties of the 1,1,1,2,2,3,3,4,4-nonafluoro-6-propoxyhexane (TE4) additive, a gamma fluorinated ether. The results show that with the introduction of TE4 additive up to 4 times higher O_2 solubility and up to 2 times higher O_2 diffusion coefficient can be achieved.

CONCLUSION

In this Perspective, the mass transfer in different regions of LABs with or without discharge products has been systematically analyzed with the aim to enhance the battery rate performance. The potential distribution of LABs is discussed not only in the bulk electrolyte but also inside the electrode; consequently, the relevant ion transfer is clearly illustrated. The results show that constructing a stable double layer plays a crucial role in the Li^+ transfer. The process of oxygen transfer is divided into three distinct stages, and each stage is briefly discussed. Further studies are needed to distinguish whether the process through the gas−liquid interface or diffusion in the liquid phase is the rate-determining step of oxygen transfer. Based on these discussions, strategies on how to improve the mass transfer in LABs are provided. Additionally, we have also pointed out that the path of mass transfer is closely related to the reaction interface when the discharge products exist. If the reaction occurs at the interface between the electrode and electrolyte, then species transfer through the discharge products will be inevitable. To this end, more efforts should be invested in the confirmation of the reaction interface, an

https://doi.org/10.1021/acsnano.4c04529
ACS Nano 2024, 18, 17361−17368

increase in conductivity of the discharge products, or the generation of soluble discharge products. This Perspective is beneficial for a systematic understanding of the mass transfer process in LABs, and it also could provide deep insight for other battery systems.

AUTHOR INFORMATION

Corresponding Authors

Xin-Bo Zhang − *State Key Laboratory of Rare Earth Resource Utilization, Changchun Institute of Applied Chemistry, Chinese Academy of Sciences, Changchun 130022, People's Republic of China;* orcid.org/0000-0002-5806-159X; Email: xbzhang@ciac.ac.cn

Gang Huang − *State Key Laboratory of Rare Earth Resource Utilization, Changchun Institute of Applied Chemistry, Chinese Academy of Sciences, Changchun 130022, People's Republic of China;* orcid.org/0000-0003-2518-8145; Email: ghuang@ciac.ac.cn

Authors

Yu-Long Liang − *Key Laboratory of Automobile Materials, Ministry of Education, Department of Materials Science and Engineering, Jilin University, Changchun 130022, People's Republic of China; State Key Laboratory of Rare Earth Resource Utilization, Changchun Institute of Applied Chemistry, Chinese Academy of Sciences, Changchun 130022, People's Republic of China*

Yue Yu − *Department of Chemistry and Waterloo Institute for Nanotechnology, University of Waterloo, Waterloo, Ontario N2L 3G1, Canada*

Zi-Wei Li − *Key Laboratory of Automobile Materials, Ministry of Education, Department of Materials Science and Engineering, Jilin University, Changchun 130022, People's Republic of China; State Key Laboratory of Rare Earth Resource Utilization, Changchun Institute of Applied Chemistry, Chinese Academy of Sciences, Changchun 130022, People's Republic of China*

Jun-Min Yan − *State Key Laboratory of Rare Earth Resource Utilization, Changchun Institute of Applied Chemistry, Chinese Academy of Sciences, Changchun 130022, People's Republic of China;* orcid.org/0000-0001-8511-3810

Complete contact information is available at: https://pubs.acs.org/10.1021/acsnano.4c04529

Author Contributions

Y.-L.L. and Y.Y. contributed equally to this work. The manuscript was written through contributions of all authors

Notes

The authors declare no competing financial interest.

ACKNOWLEDGMENTS

This work was financially supported by the National Key R&D Program of China (2021YFF0500600), National Natural Science Foundation of China (U23A20575, U22A20437, 52171194), New Cornerstone Science Foundation through the XPLORER PRIZE, CAS Project for Young Scientists in Basic Research (YSBR-058), and National Natural Science Foundation of China Outstanding Youth Science Foundation of China (Overseas).

REFERENCES

(1) Loganathan, M. K.; Mishra, B.; Tan, C. M.; Kongsvik, T.; Rai, R. N. Multi-Criteria Decision Making (MCDM) for the Selection of Li-Ion Batteries Used in Electric Vehicles (EVs). *Mater. Today: Proc.* **2021**, *41*, 1073−1077.

(2) Adepoju, A. A.; Williams, Q. L. High C-Rate Performance of $LiFePO_4$/Carbon Nanofibers Composite Cathode for Li-Ion Batteries. *Curr. Appl. Phys.* **2020**, *20*, 1−4.

(3) Zeng, X.; Li, M.; Abd El-Hady, D.; Alshitari, W.; Al-Bogami, A. S.; Lu, J.; Amine, K. Commercialization of Lithium Battery Technologies for Electric Vehicles. *Adv. Energy Mater.* **2019**, *9*, 1900161.

(4) Eftekhari, A. Lithium-Ion Batteries with High Rate Capabilities. *ACS Sustainable Chem. Eng.* **2017**, *5*, 2799−2816.

(5) Zhang, L.; Jiang, J.; Zhang, C.; Wu, B.; Wu, F. High-Rate Layered Lithium-Rich Cathode Nanomaterials for Lithium-Ion Batteries Synthesized with the Assist of Carbon Spheres Templates. *J. Power Sources* **2016**, *331*, 247−257.

(6) Chang, Z.-R.; Liu, Y.; Tang, H.-W.; Yuan, X.-Z.; Wang, H. DMSO-Assisted Liquid-Phase Synthesis of $LiFePO_4$/C Nanocomposites with High-Rate Cycling As Cathode Materials for Lithium Ion Batteries. *Electrochem. Solid-State Lett.* **2011**, *14*, A90.

(7) Huang, C. Y.; Kuo, T. R.; Yougbare, S.; Lin, L. Y. Design of $LiFePO_4$ and Porous Carbon Composites with Excellent High-Rate Charging Performance for Lithium-Ion Secondary Battery. *J. Colloid Interface Sci.* **2022**, *607*, 1457−1465.

(8) Yuan, B.; Wen, K.; Chen, D.; Liu, Y.; Dong, Y.; Feng, C.; Han, Y.; Han, J.; Zhang, Y.; Xia, C.; Sun, A.; He, W. Composite Separators for Robust High Rate Lithium Ion Batteries. *Adv. Funct. Mater.* **2021**, *31*, 2101420.

(9) Kwak, W. J.; Rosy; Sharon, D.; Xia, C.; Kim, H.; Johnson, L. R.; Bruce, P. G.; Nazar, L. F.; Sun, Y. K.; Frimer, A. A.; Noked, M.; Freunberger, S. A.; Aurbach, D. Lithium-Oxygen Batteries and Related Systems: Potential, Status, and Future. *Chem. Rev.* **2020**, *120*, 6626−6683.

(10) Read, J.; Mutolo, K.; Ervin, M.; Behl, W.; Wolfenstine, J.; Driedger, A.; Foster, D. Oxygen Transport Properties of Organic Electrolytes and Performance of Lithium/Oxygen Battery. *J. Electrochem. Soc.* **2003**, *150*, A1351.

(11) Read, J. Characterization of the Lithium/Oxygen Organic Electrolyte Battery. *J. Electrochem. Soc.* **2002**, *149*, A1190.

(12) Gittleson, F. S.; Jones, R. E.; Ward, D. K.; Foster, M. E. Oxygen Solubility and Transport in Li-Air Battery Electrolytes: Establishing Criteria and Strategies for Electrolyte Design. *Energy Environ. Sci.* **2017**, *10*, 1167−1179.

(13) Wang, F.; Li, X.; Hao, X.; Tan, J. Review and Recent Advances in Mass Transfer in Positive Electrodes of Aprotic Li-O_2 Batteries. *ACS Appl. Energy Mater.* **2020**, *3*, 2258−2270.

(14) Gavish, N.; Promislow, K. Dependence of the Dielectric Constant of Electrolyte Solutions on Ionic Concentration: A Microfield Approach. *Phys. Rev. E* **2016**, *94*, 012611.

(15) Wang, P.; Anderko, A. Computation of Dielectric Constants of Solvent Mixtures and Electrolyte Solutions. *Fluid Phase Equilib.* **2001**, *186*, 103−122.

(16) Bard, A. J.; Faulkner, L. R. Double-Layer Structure and Absorption. In *Electrochemical Methods: Fundamentals and Applications*; Harris, D., Swain, E., Robey, C., Aiello, E., Eds.; Wiley: 2021; pp 534−579.

(17) Rezaei Niya, S. M.; Andrews, J. On Charge Distribution and Storage in Porous Conductive Carbon Structure. *Electrochim. Acta* **2022**, *402*, 139534.

(18) Kube, A.; Bienen, F.; Wagner, N.; Friedrich, K. A. Wetting Behavior of Aprotic Li-Air Battery Electrolytes. *Adv. Mater. Interfaces* **2022**, *9*, 2101569.

(19) Zhang, X.; Valeriote, E. Galvanic Protection of Steel and Galvanic Corrosion of Zinc under Thin Layer Electrolytes. *Corros. Sci.* **1993**, *34*, 1957−1972.

(20) Zhang, P.; Zhao, Y.; Zhang, X. Functional and Stability Orientation Synthesis of Materials and Structures in Aprotic Li-O_2 Batteries. *Chem. Soc. Rev.* **2018**, *47*, 2921−3004.
(21) Park, J.-B.; Hassoun, J.; Jung, H.-G.; Kim, H.-S.; Yoon, C. S.; Oh, I.-H.; Scrosati, B.; Sun, Y.-K. Influence of Temperature on Lithium-Oxygen Battery Behavior. *Nano Lett.* **2013**, *13*, 2971−2975.
(22) Nishikami, Y.; Konishi, T.; Omoda, R.; Aihara, Y.; Oyaizu, K.; Nishide, H. Oxygen-Enriched Electrolytes Based on Perfluorochemicals for High-Capacity Lithium-Oxygen Batteries. *J. Mater. Chem. A* **2015**, *3*, 10845−10850.
(23) Truesdale, G.; Downing, A. Solubility of Oxygen in Water. *Nature* **1954**, *173*, 1236−1236.
(24) Liu, T.; Vivek, J. P.; Zhao, E. W.; Lei, J.; Garcia-Araez, N.; Grey, C. P. Current Challenges and Routes Forward for Nonaqueous Lithium-Air Batteries. *Chem. Rev.* **2020**, *120*, 6558−6625.
(25) Hummelshoj, J. S.; Luntz, A. C.; Norskov, J. K. Theoretical Evidence for Low Kinetic Overpotentials in Li-O_2 Electrochemistry. *J. Chem. Phys.* **2013**, *138*, 034703.
(26) Zhang, Z.; Xiao, X.; Yu, W.; Zhao, Z.; Tan, P. Reacquainting the Sudden-Death and Reaction Routes of Li-O_2 Batteries by Ex Situ Observation of Li_2O_2 Distribution Inside a Highly Ordered Air Electrode. *Nano Lett.* **2022**, *22*, 7527−7534.
(27) Prehal, C.; Samojlov, A.; Nachtnebel, M.; Lovicar, L.; Kriechbaum, M.; Amenitsch, H.; Freunberger, S. A. In Situ Small-Angle X-Ray Scattering Reveals Solution Phase Discharge of Li-O_2 Batteries With Weakly Solvating Electrolytes. *Proc. Natl. Acad. Sci. U.S.A.* **2021**, *118*, e2021893118.
(28) Kraytsberg, A.; Ein-Eli, Y. The Impact of Nano-Scaled Materials on Advanced Metal-Air Battery Systems. *Nano Energy* **2013**, *2*, 468−480.
(29) Xiao, J.; Mei, D.; Li, X.; Xu, W.; Wang, D.; Graff, G. L.; Bennett, W. D.; Nie, Z.; Saraf, L. V.; Aksay, I. A.; Liu, J.; Zhang, J. G. Hierarchically Porous Graphene As a Lithium-Air Battery Electrode. *Nano Lett.* **2011**, *11*, 5071−5078.
(30) Li, Y.; Wang, J.; Li, X.; Geng, D.; Li, R.; Sun, X. Superior Energy Capacity of Graphene Nanosheets for a Nonaqueous Lithium-Oxygen Battery. *Chem. Commun.* **2011**, *47*, 9438−9440.
(31) Gaya, C.; Yin, Y.; Torayev, A.; Mammeri, Y.; Franco, A. A. Investigation of Bi-Porous Electrodes for Lithium Oxygen Batteries. *Electrochim. Acta* **2018**, *279*, 118−127.
(32) Leng, L.; Zeng, X.; Chen, P.; Shu, T.; Song, H.; Fu, Z.; Wang, H.; Liao, S. A Novel Stability-Enhanced Lithium-Oxygen Battery with Cellulose-Based Composite Polymer Gel As the Electrolyte. *Electrochim. Acta* **2015**, *176*, 1108−1115.
(33) Kim, B. G.; Kim, J. S.; Min, J.; Lee, Y. H.; Choi, J. H.; Jang, M. C.; Freunberger, S. A.; Choi, J. W. A Moisture- and Oxygen-Impermeable Separator for Aprotic Li-O_2 Batteries. *Adv. Funct. Mater.* **2016**, *26*, 1747−1756.
(34) Padbury, R.; Zhang, X. Lithium-Oxygen Batteries-Limiting Factors That Affect Performance. *J. Power Sources* **2011**, *196*, 4436−4444.
(35) Li, C.; Yu, Z.; Liu, H.; Chen, K. High Surface Area $LaMnO_3$ Nanoparticles Enhancing Electrochemical Catalytic Activity for Rechargeable Lithium-Air Batteries. *J. Phys. Chem. Solids* **2018**, *113*, 151−156.
(36) Li, Y.; Li, X.; Geng, D.; Tang, Y.; Li, R.; Dodelet, J.-P.; Lefèvre, M.; Sun, X. Carbon Black Cathodes for Lithium Oxygen Batteries: Influence of Porosity and Heteroatom-Doping. *Carbon* **2013**, *64*, 170−177.
(37) Jiang, J.-Z.; Zhang, S.; Fu, X.-L.; Liu, L.; Sun, B.-M. Review of Gas-Liquid Mass Transfer Enhancement by Nanoparticles from Macro to Microscopic. *Heat Mass Transfer* **2019**, *55*, 2061−2072.
(38) Wan, H.; Bai, Q.; Peng, Z.; Mao, Y.; Liu, Z.; He, H.; Wang, D.; Xie, J.; Wu, G. A High Power Li-Air Battery Enabled by a Fluorocarbon Additive. *J. Mater. Chem. A* **2017**, *5*, 24617−24620.

https://doi.org/10.1021/acsnano.4c04529
ACS Nano 2024, 18, 17361−17368